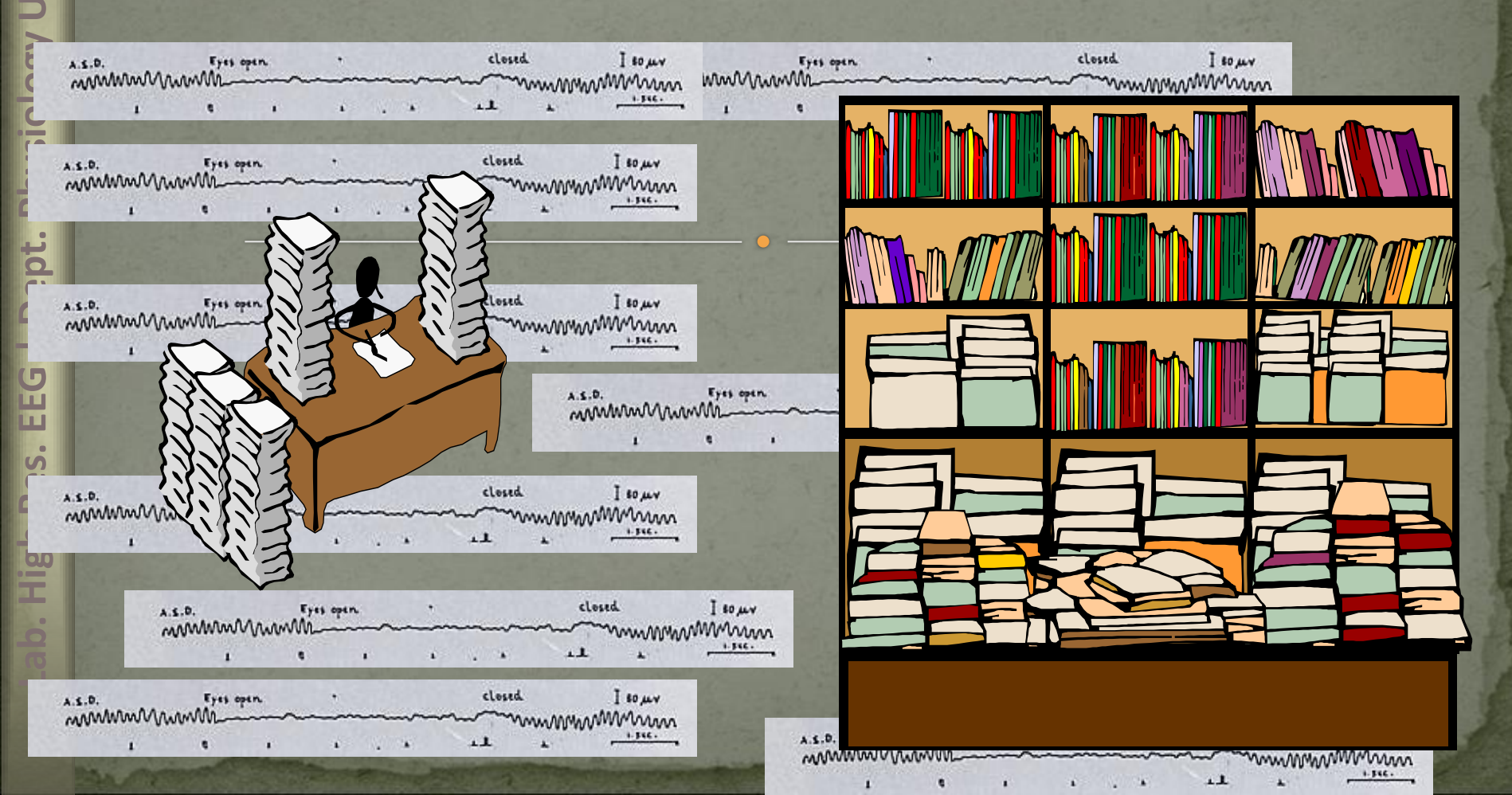
The spatial analysis of high resolution EEG data

Prof. Fabio Babiloni
Laboratory of High Resolution EEG
University of Rome "Sapienza"

The standard EEG heritage



Human tissues produce measurable potential differences

In 1849 the German physiologist Emil Heinrich Du Bois-Reymond first reported the detection of minute electrical discharges created by the contraction of the muscles in his arms



In 1880 Waller first measure the EKG in dogs

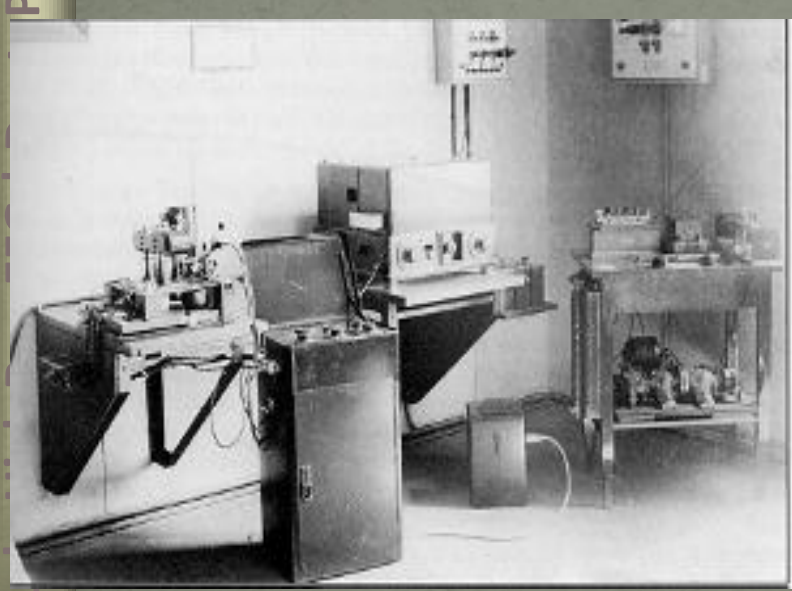


....and humans

Human brain produces measurable signals on the scalp

Hans Berger in 1929 produced the first report on the measurement of electrical activity **in man** over the scalp surface

He hoped that EEG could represent a sort of "window on the mind"



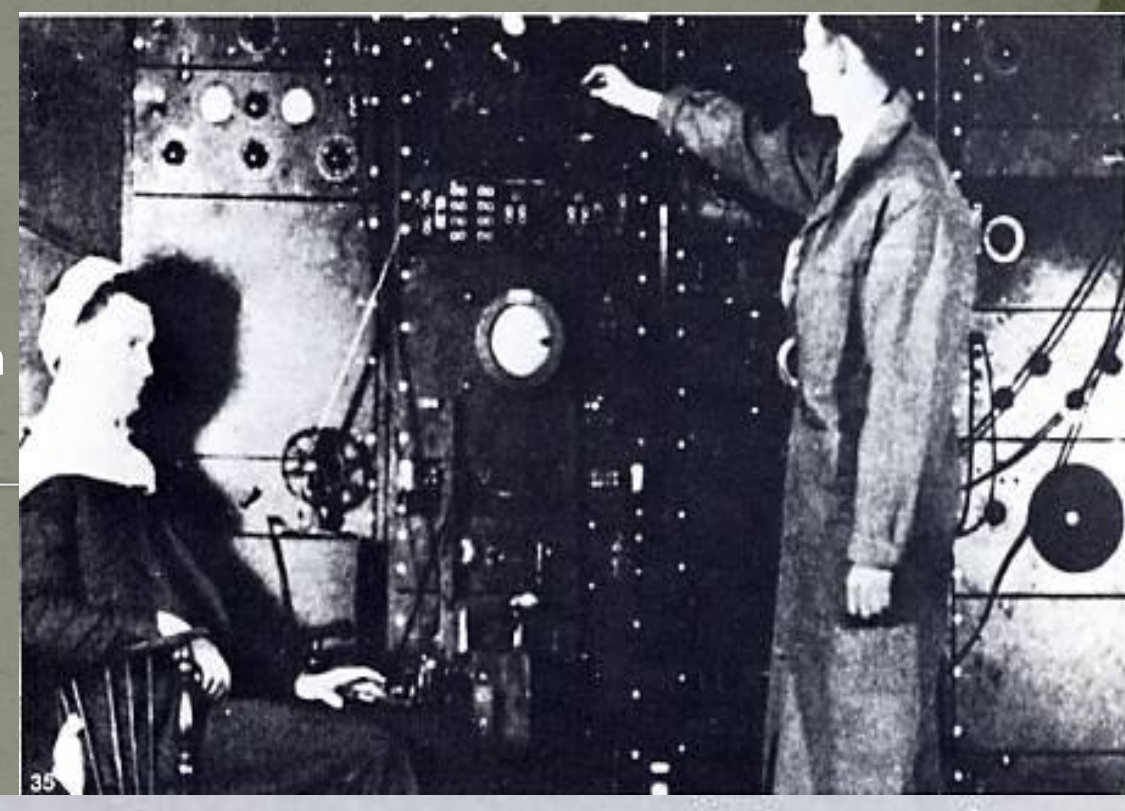




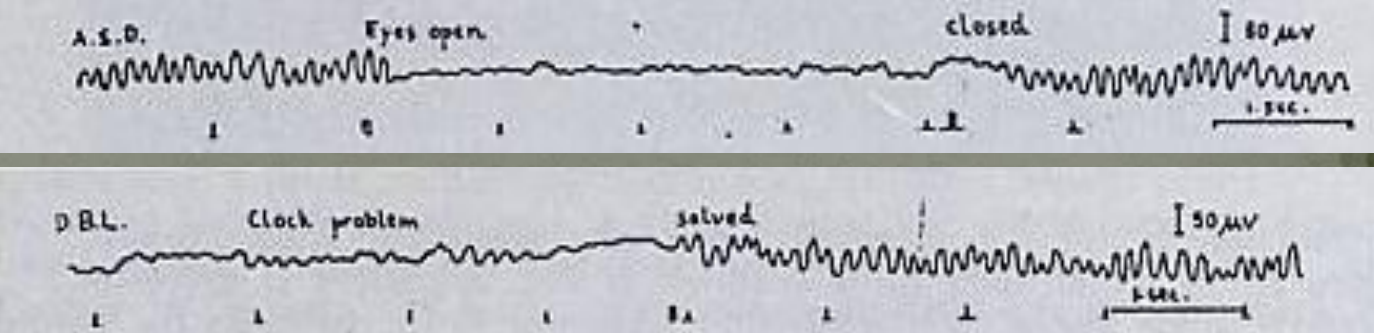
Berger's equipment

1-EEG channel device at the Harvard Medical School, 1934

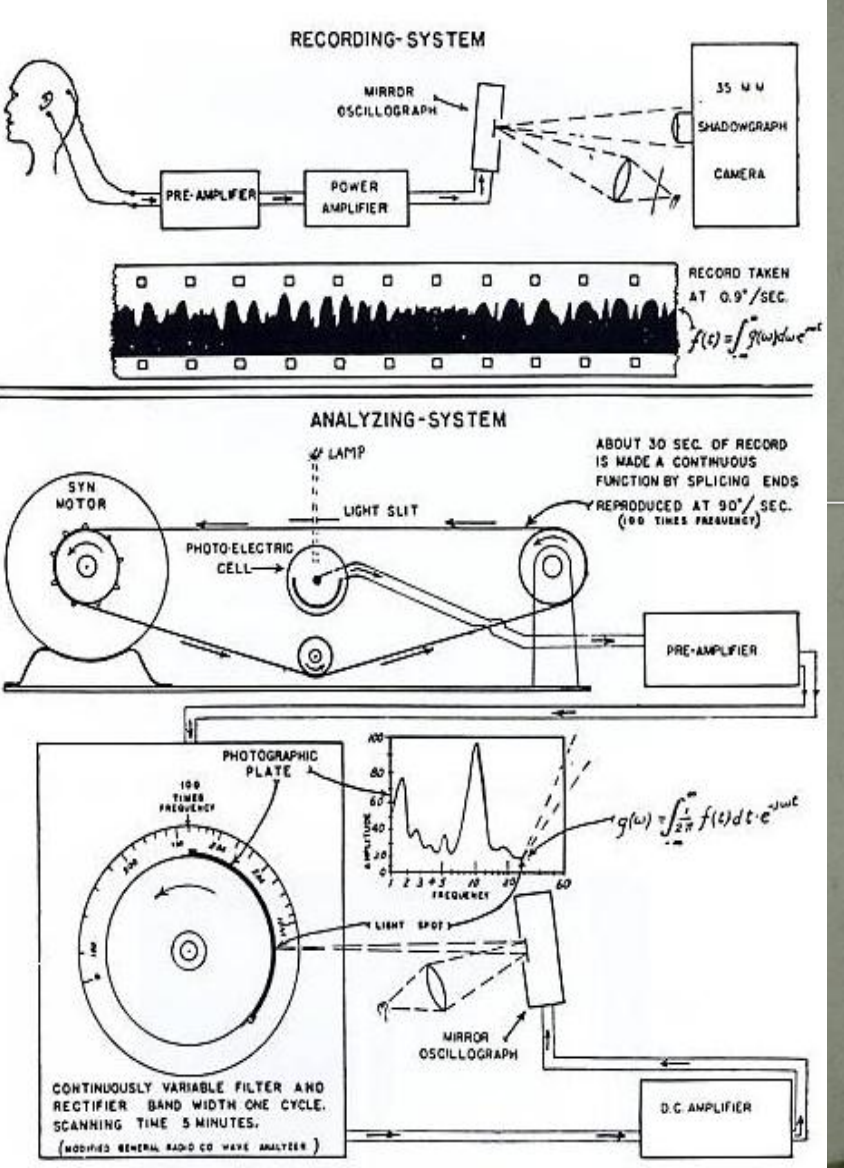
- EEG was performed at the Davis laboratory in Harvard
- A crown of saline soaked cotton bandage for ground and an hyperdermic needle in the vertex



Eyes open and closed Mental calculation



Computational tools to improve understanding of brain function



Grass and Gibbs, The Fourier Transform of the EEG, J. of Neurophysiology 1938



Gibbs, time-varying spectra, 1941,35 years before Bickford's CSA

Some old EEG devices



Cet aniemble E.E.G. - REEGA VI - BLOC se recommande par sa technique et la securité de son service.

E est uns approve dans les numbres. L'aberatores E E.G. ou il est actuellement utilisé. ARTEX+FRANCE

Circa 1949 France

Physiology

O

O

po

.



Circa 1950 U.S.A.

71



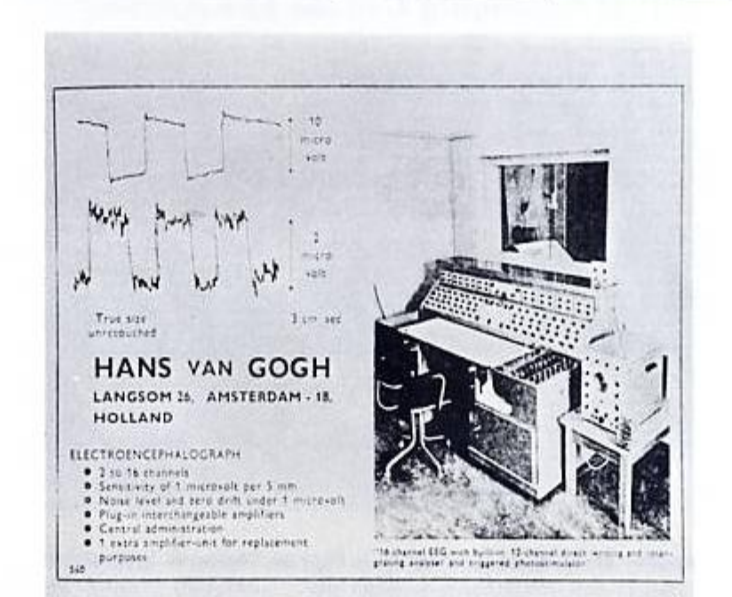




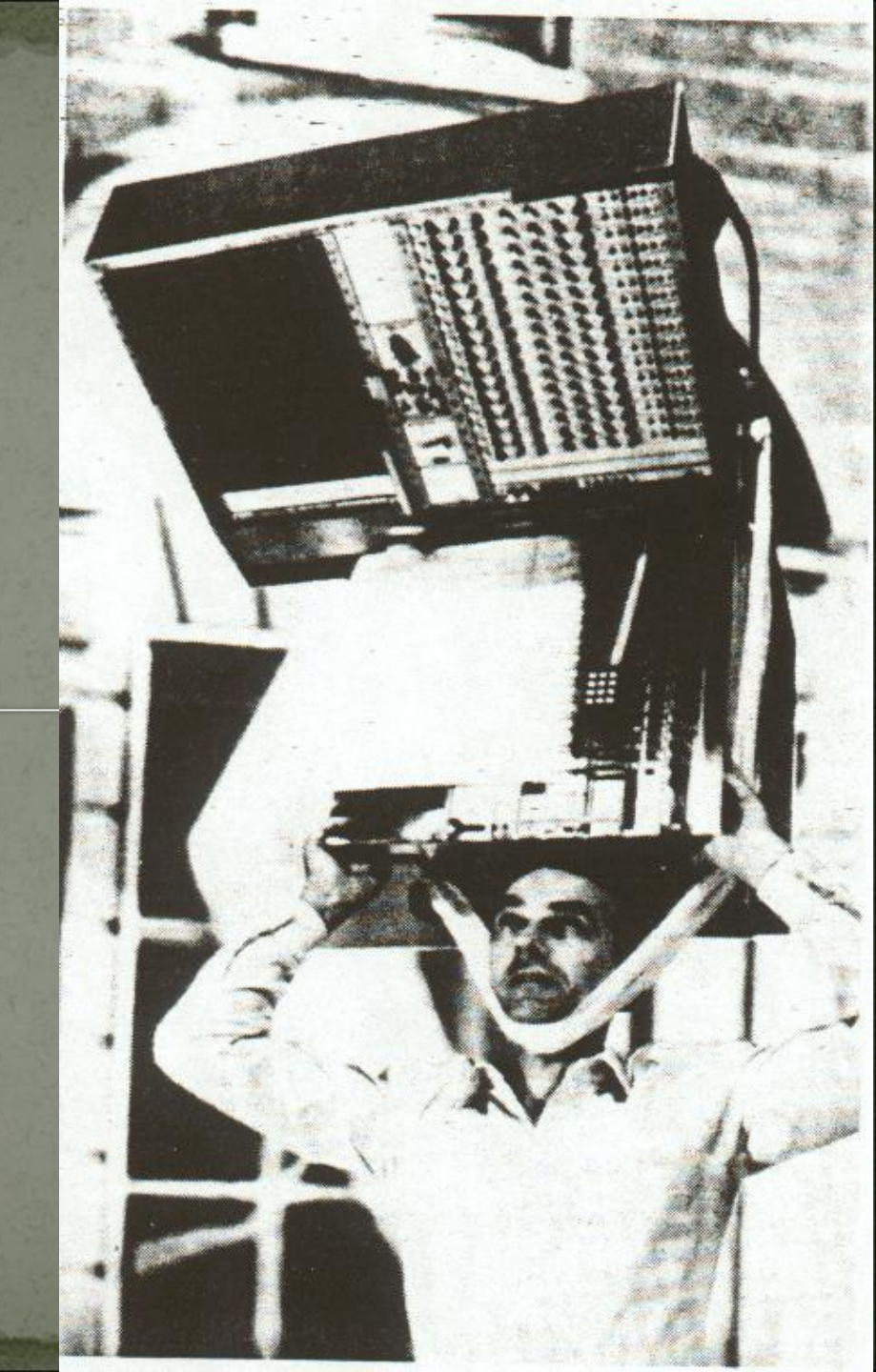
ST. ALBANE HESTPORDSHIRE ENGLAND







....and the portable one



Dept.

Why the conventional EEG is not largely used in neuroscience?

In 1929 Berger discovers the human EEG. After more than 70 years, EEG is not largely used in science apart for localization studies in epilepsy

- - Dependence of data on the electrical reference used
- Factors limiting the utility of the EEG are

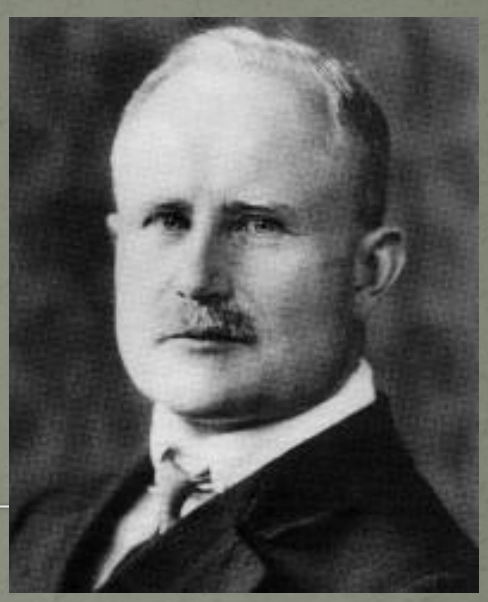
 Spatial blur

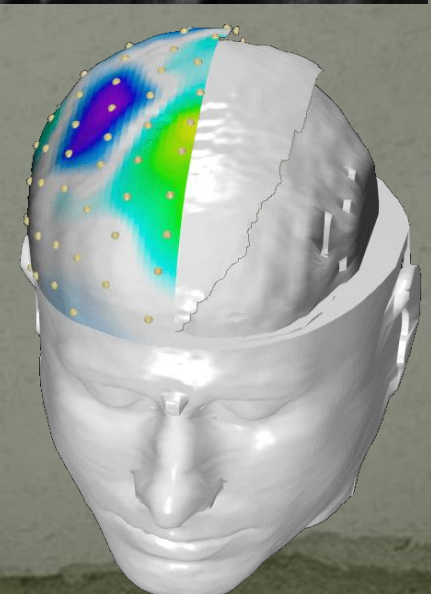
 Dependence of data on the electrical reference.

 Spatial aliasing (insufficient number of electrical reference). Spatial aliasing (insufficient number of electrodes) used

Now, with the aid of available computational power and Magnetic Resonance head images, the EEG can became a science.

See further for explanations



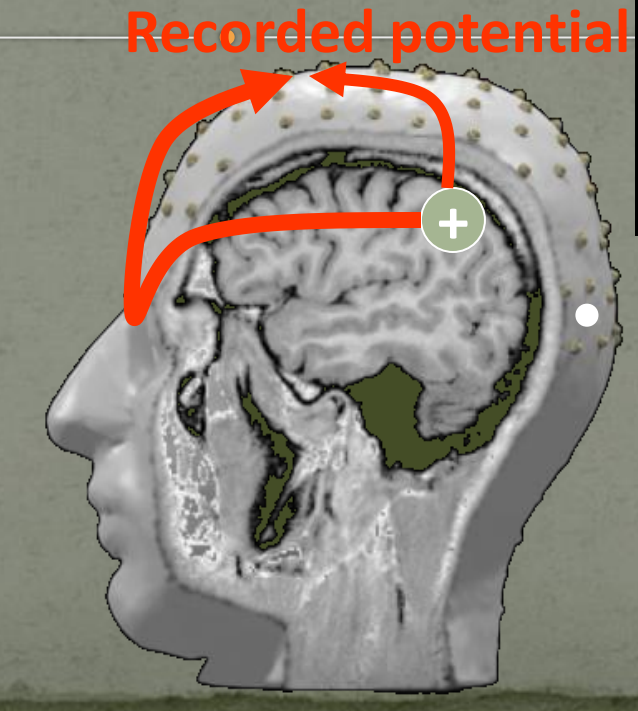


Spatial blur of the EEG

An accurate modelling of the structures allows to treat efficiently the problems of standard EEG

Poorly conductive skull spatially blurs scalp potentials

Electrical reference depresses near sources

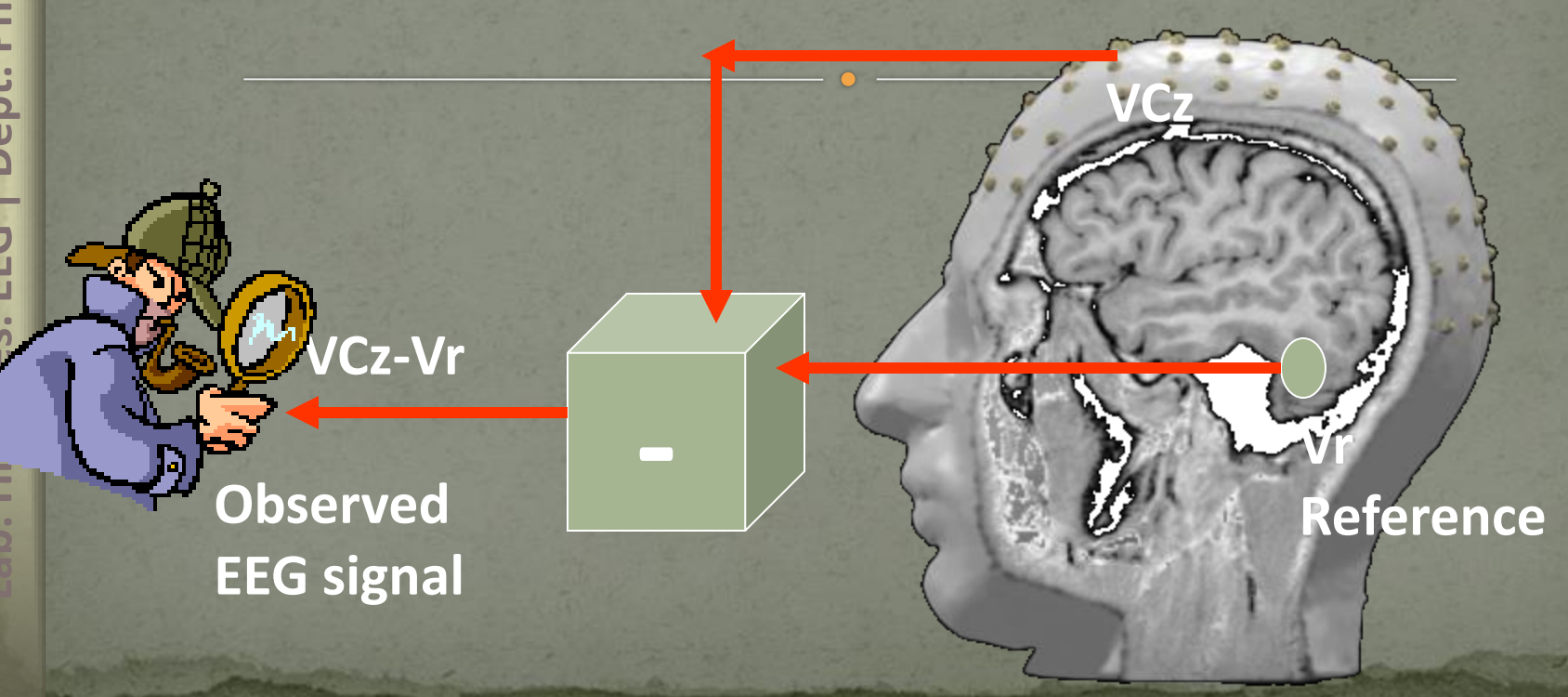


Furthermore, eye and ear holes provide shunt paths for the cerebral currents

EEG Spatial Blur Induced by the Electrical Reference

Spatial blurring is increased by the variation of the electrical reference used in EEG recording

The variation electrical reference acts as a spatial filter that may enhance the activity of some neural sources and depress the activity of the others



Variations of electrical reference changes the spectral profile of the EEG traces an its derived measures

High resolution EEG

What does it measure?

extracellular currents at cortical and sub-cortical levels of synchronized neuronal populations

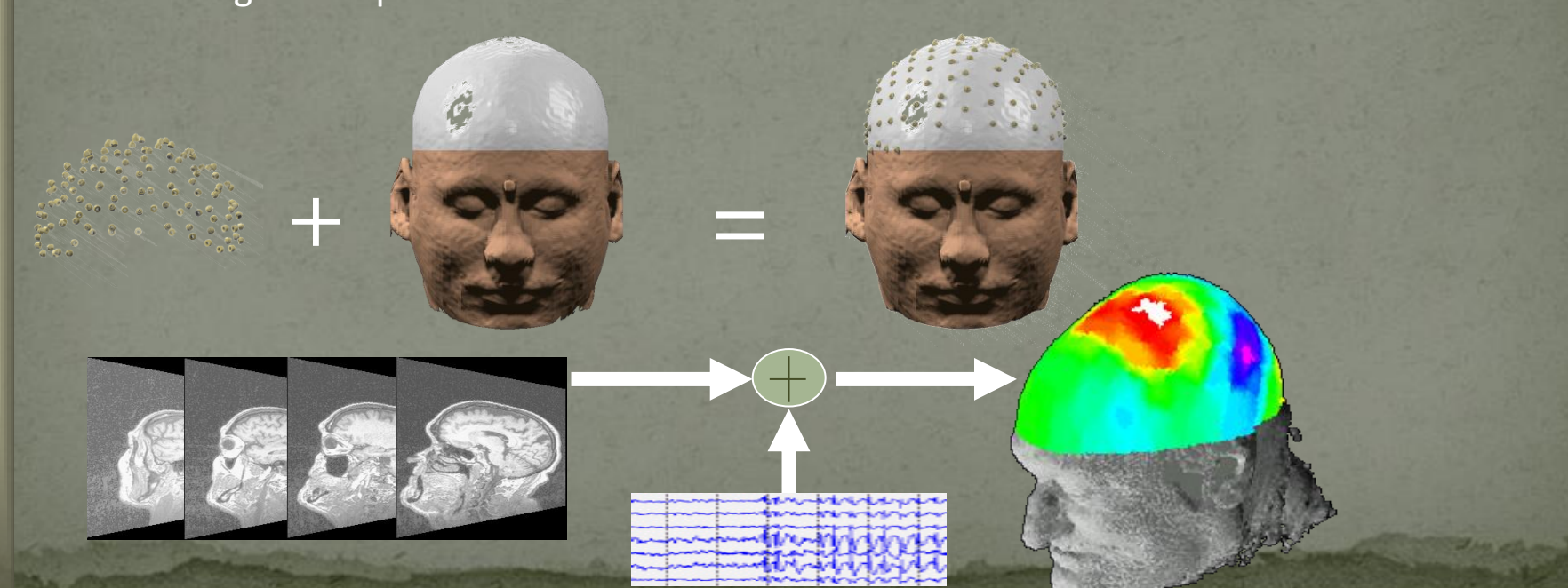
High temporal resolution (msec scale)

Low-moderate spatial resolution

EEG: 2-3 cm

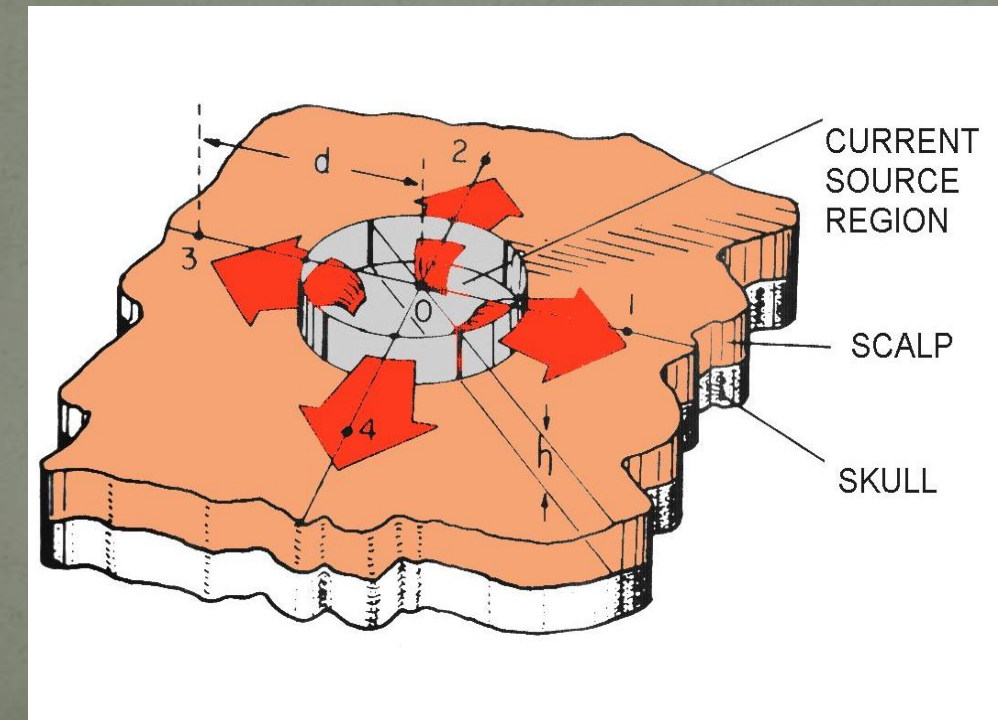
Key factors in high resolution EEG

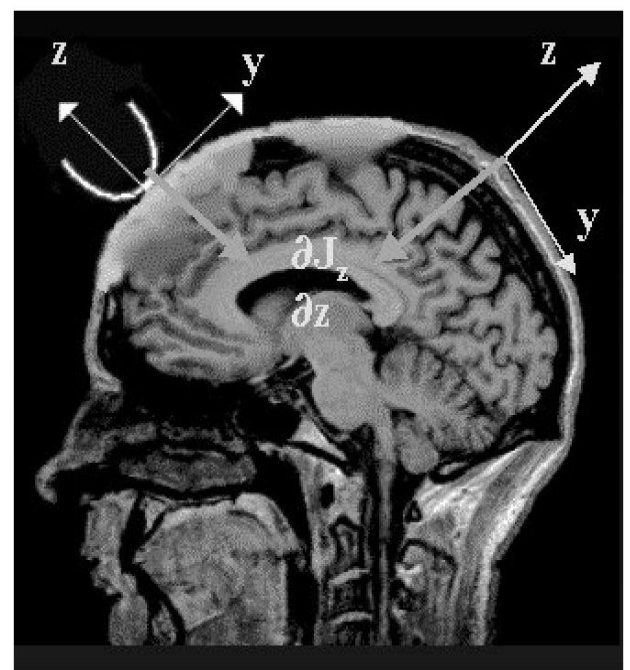
64-128 electrodes, realistic reconstruction of head volume conductor, spatial deblurring techniques



EEG spatial enhancement by SL

- The SL estimation acts as a spatial highpass or bandpass filter
- Increasing the number of electrodes improves the estimation of SL





Improving the spatial details of the EEG by the surface Laplacian (SL)

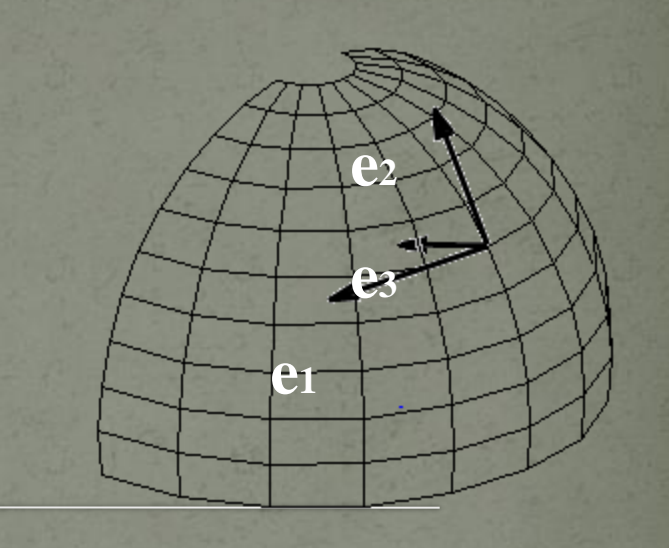
- The SL is estimated by computing the second order spatial derivatives of the potential distribution over a scalp model
- The SL provides an estmate of the radial current density (J) flowing from the scalp into the scalp
- The SL estimation acts as a spatial highpass or bandpass filter that:
 - Enhances the activity generated from local (cortical) sources and depresses the activity originated from distant (subcortical) sources
 - Provides reference-free EEG
- Increasing the number of electrodes sampling the potential distribution improves the estimation of SI

Surface Laplacian

$$\nabla \cdot J = 0$$
 $J = -\sigma(e_1, e_2)E$ $E = -\nabla \cdot V$

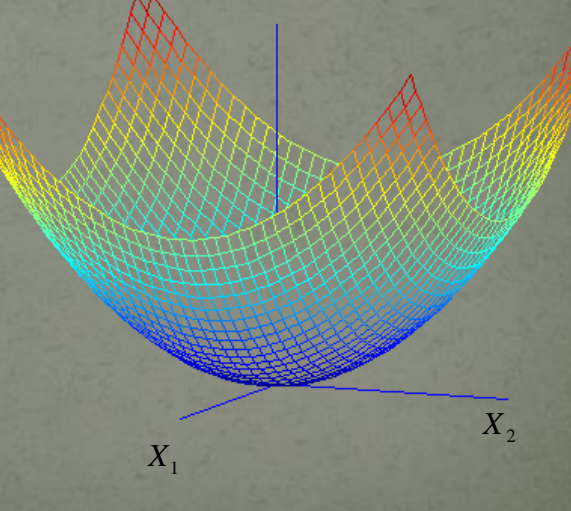
$$I = \frac{\partial J_3}{\partial e_3} = -\left(\frac{\partial J_1}{\partial e_1} + \frac{\partial J_2}{\partial e_2}\right) = -\sigma(e_1, e_2) \left(\frac{\partial^2 V}{\partial e_1^2} + \frac{\partial^2 V}{\partial e_2^2}\right)$$

$$\left(\frac{\partial^{2}}{\partial e_{1}^{2}} + \frac{\partial^{2}}{\partial e_{2}^{2}}\right) [V(x_{1}, x_{2})] \implies (X_{1}^{2} + X_{2}^{2}) \cdot V(X_{1}, X_{2})$$



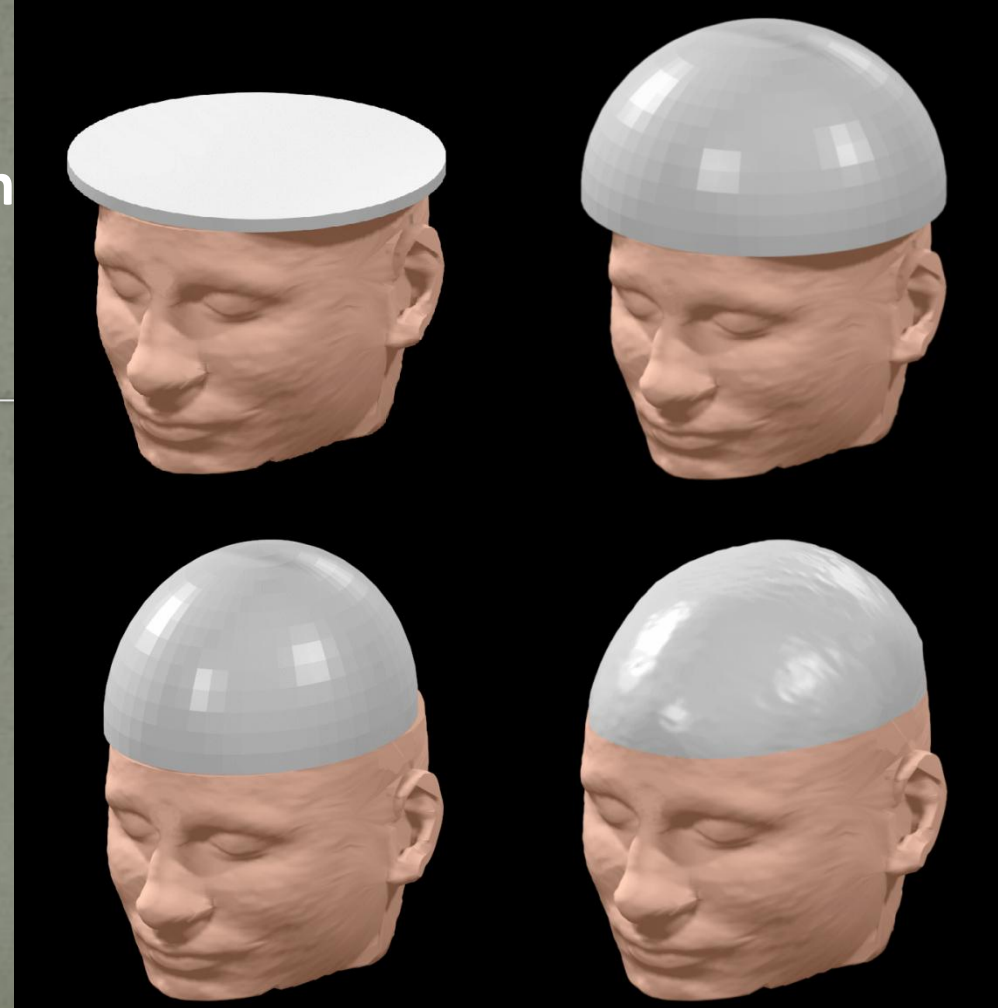
We need an analytical description of:

- scalp
- potenzial



Which scalp surface models we would like to assume for the computation of SL?

Planar, Hjorth 1980



Ellipsoidal Law et al., 1993

Spherical,
Perrin et al,
1989

Realistic

Since 20 years ago the EEG data can be visualized in this way

Since 10 years ago the data regarding the SL on the spherical head surface can be visualized in this way

Potential

Spherical SL

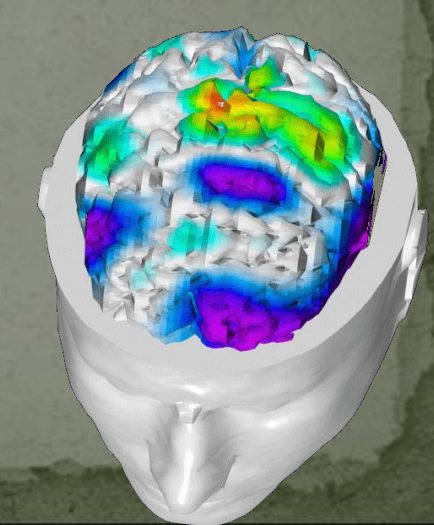
Now, by computing the RL on the realistic head structures it is possible to visualize the cerebral activity on the appropriate subject scalp.

EEG

Res.

Realistic SL

Furthermore, a correspondence between scalp activity and underlying cortical activity can be issued



Spherical splines for interpolation and estimation of surface Laplacian

- Generic position E on the sphere
- Ei are the generic electrodes positions (i=1, N)
- $V(E) = c0 + \Sigma i \operatorname{cig}(\cos(E,Ei))$
- C' = [c1,...,cN] is found as solution of

$$G C + T c0 = Z$$

$$Tt C = 0$$

Having T' = [1...,1]; Z' = [z1,...zN] and the G matrix as Gij = g(cos(Ei,Ej)) with Pn associate Legendre polynomials

$$g(x) = \left(\frac{1}{4\pi}\right) \sum_{n=1}^{\infty} \left(\frac{2n+1}{n^{m}(n+1)^{m}}\right) P_n(x)$$

$$(n+1) Pn+1(x) = (2n+1) x Pn(x) - n Pn-1(x)$$

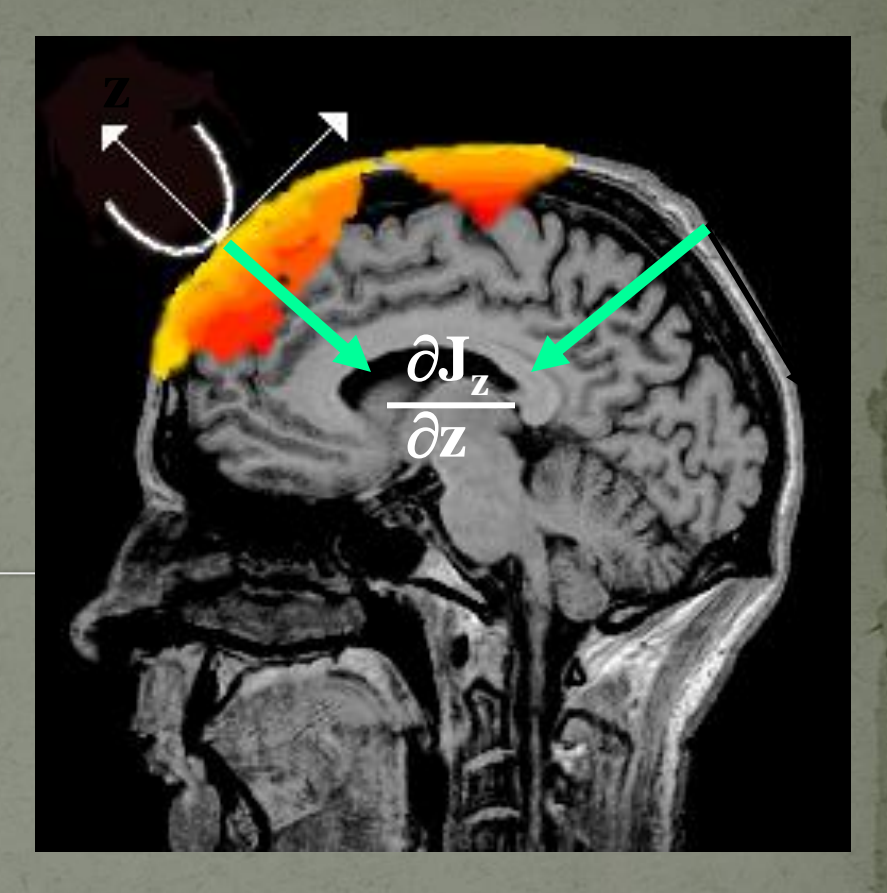
P0 = 1

Spherical splines for the estimation of the surface laplacian

- The associate Legendre polinomials are eigenfunction of the nabla operator on the sphere (Laplace-Beltrami)
- Hence the estimation of the surface Laplacian is obtained by applying the nabla on the spherical splines formula for the surface potential
- The key issue is that the solution of the linear system for the coefficient estimation is possible as described in Perrin et al, EEG J, 1990 (and successive correction).

Realistic Surface Laplacian

- A new formulation of the surface Laplacian became necessary using realistic scalp surface modeling
- The orientation of the reference system changes from point to point on a realistic surface model instead to be fixed as in the other scalp model



Non orthogonal curvilinear reference system on the realistic scalp surface

Realistic Surface Laplacian

$$x = u, y = v \text{ and } z = f(u,v)$$
 (1)

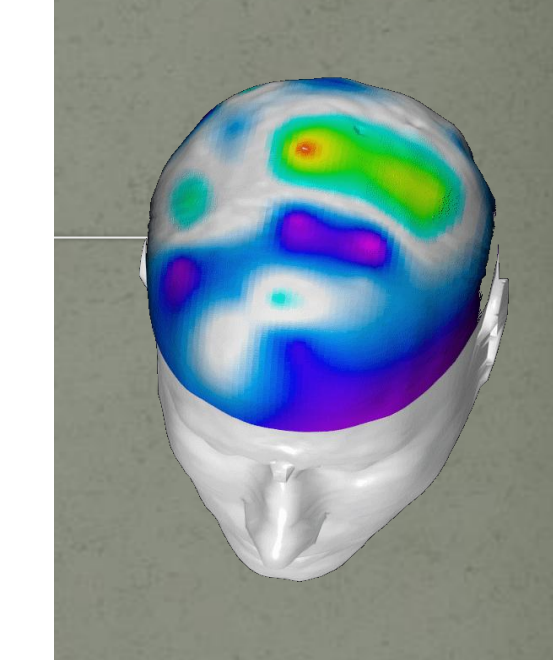
is a curvilinear coordinate system on Ω , and f(u,v) a function whose second order partial derivatives exist and are continuous. If V(u,v) is the potential distribution on Ω , the SL of V(u,v) is given by the following equation:

$$\nabla^{2}V(u,v) = \frac{1}{\sqrt{g}} \left(\frac{\partial}{\partial u} \left(\sqrt{g} \right) \left(g^{11} \frac{\partial V}{\partial u} + g^{12} \frac{\partial V}{\partial v} \right) + \frac{\partial}{\partial v} \left(\sqrt{g} \right) \left(g^{21} \frac{\partial V}{\partial u} + g^{22} \frac{\partial V}{\partial v} \right) \right)$$
(2)

where the components of the metric tensor are computed as follows:

$$g = 1 + \left(\frac{\partial f}{\partial u}\right)^2 + \left(\frac{\partial f}{\partial v}\right)^2; g^{11} = \frac{1 + \left(\frac{\partial f}{\partial v}\right)^2}{g}$$

$$g^{12} = g^{21} = \frac{-\frac{\partial f}{\partial u} \frac{\partial f}{\partial v}}{g}; g^{22} = \frac{1 + \left(\frac{\partial f}{\partial u}\right)^2}{g}.$$
 (3)



This spline function interpolates values V(x,y,z) from the potential values $Vi(x_i, y_i, z_i)$ measured on the scalp surface model as follows:

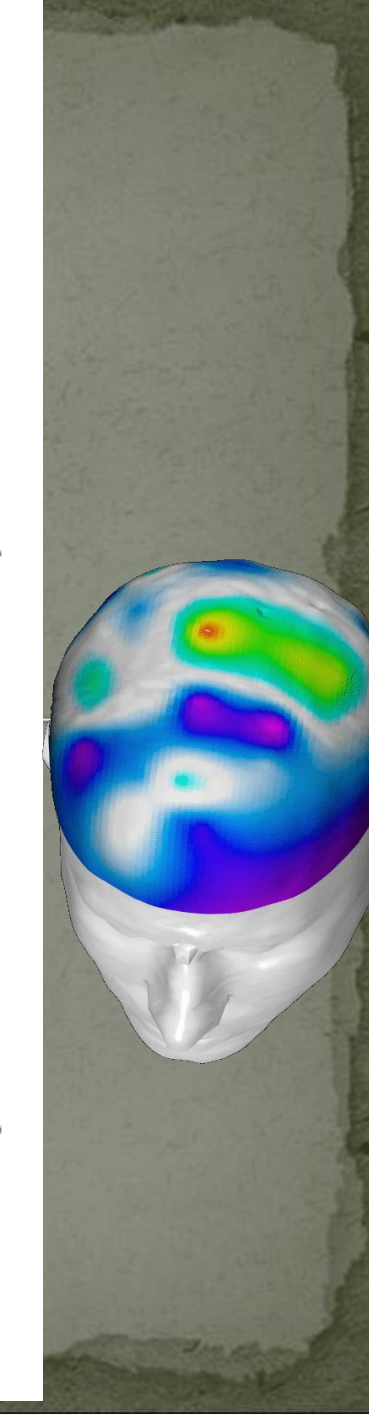
$$Vm(x,y,z) = \sum_{i=1}^{N} t_i H_{m-1}(x-x_i, y-y_i, z-z_i) + R_{m-1}(x,y,z)$$
(4)

where m (spline order) is equal to 3, N is the number of surface samples used to measure the potential distribution, and the t_i coefficients are the unknowns. The R_{m-1} function is defined by:

$$R_{m-1}(x,y,z) = \sum_{d=0}^{m-1} \sum_{k=0}^{d} \sum_{g=0}^{k} r_{dkg} x^{d-k} y^{k-g} z^{g}$$
 (5)

where r_{dkg} coefficients are the unknowns, and the H_{m-1} is defined by:

$$Hm - 1(a,b,c) = (a^2 + b^2 + c^2)^{(2m-3)/2}$$
 (6)



The t_i and r_{dkg} coefficients are obtained by:

$$(H + \lambda I) \cdot T + F \cdot R = V$$
$$F' \cdot T = 0$$

where the H, R, T, V and F arrays are defined by:

$$H = (h_{ij}) = H_{m-1}(x_i - x_j, y_i - y_j, z_i - z_j)$$
 (8)

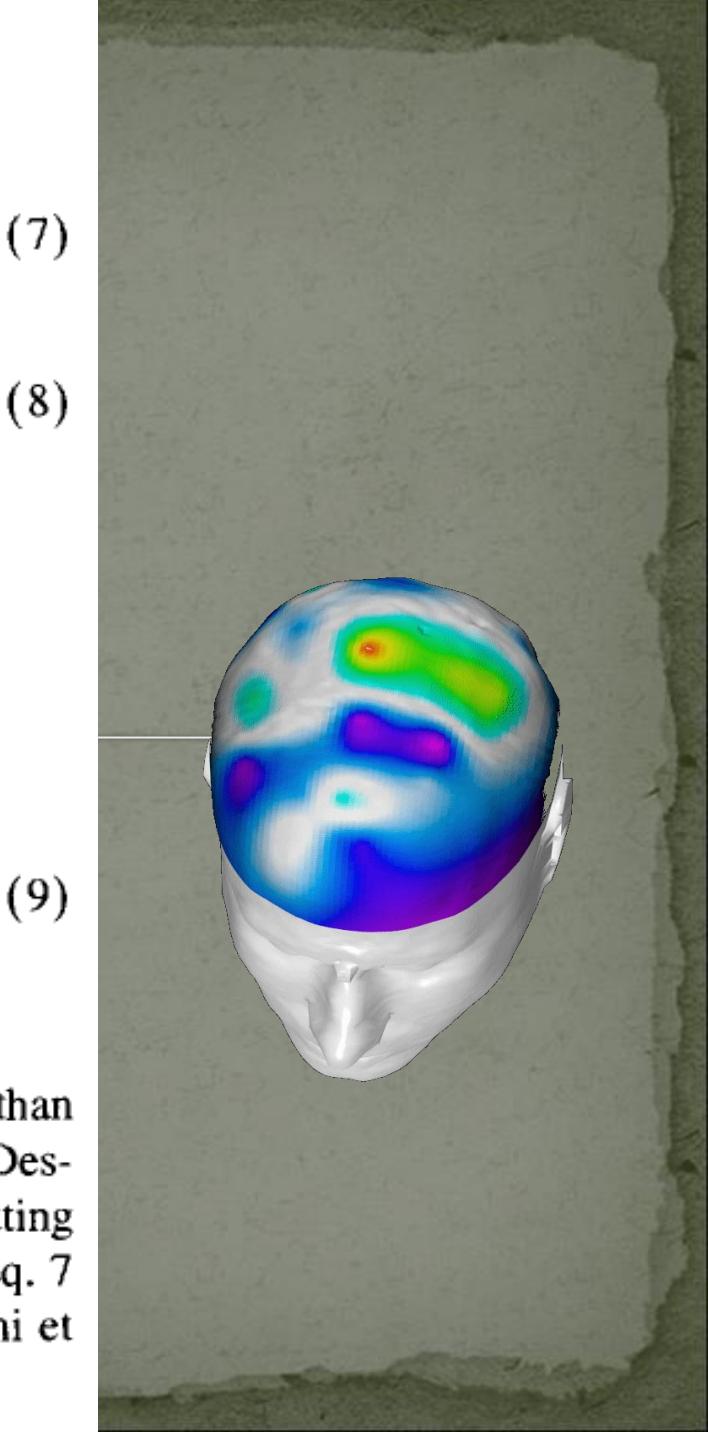
$$R^t = \begin{pmatrix} r_{00} & r_{01} & r_{11} & \cdots & r_{m-1 m-1} \end{pmatrix}$$

$$T^t = \begin{pmatrix} t_1 & t_2 & t_3 & \cdots & t_n \end{pmatrix}$$

$$V' = \begin{pmatrix} v_1 & v_2 & v_3 & \cdots & v_n \end{pmatrix}$$

$$F = \begin{cases} 1 & x_1 & y_1 & z_1 & \cdots \\ \vdots & \vdots & \ddots & \vdots \\ \vdots & \vdots & \ddots & \vdots \\ 1 & x_n & y_n & z_n & \cdots \end{cases}, \tag{9}$$

and λ was the term used to approximate rather than interpolate the potential distribution (Harder and Desmarais, 1972). The SL estimates were improved by setting an appropriate value of λ with a tuning procedure in Eq. 7 (Harder and Desmarais, 1972; Le et al., 1994; Babiloni et al., 1995).



Realistic Surface Laplacian

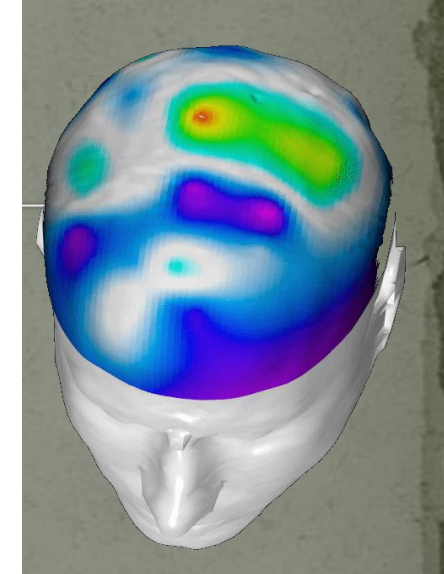
models the scalp surface in terms of Cartesian coordinates of points of the real scalp (x_r, y_r, z_r) , and in terms of location of the interpolated scalp points (x_r, y_r, z_s) by:

$$z_{s} = f(x_{r}, y_{r}) = \sum_{i=1}^{N} p_{i} K_{m-1}(x_{r} - x_{i}, y_{r} - y_{i}) + Q_{m-1}(x_{r}, y_{r})$$

$$(10)$$

where m (spline order) is equal to 2 and N is the number of points of the set S. $Q_{m-1}(x,y)$ and $K_{m-1}(x,y)$ functions are described as follows:

$$Q_{m-1}(x,y) = \sum_{d=0}^{m-1} \sum_{k=0}^{d} q_{kd} x^{d-k} y^k$$
 (11)



$$K_{m-1}(s,t) = (s^2 + t^2)^{m-1} \log(s^2 + t^2 + w^2)$$
 (12)

 $p_i s$ and $q_{ij} s$ are obtained solving the following linear equation system:

$$(K + \omega I) \cdot P + E \cdot Q = Z$$

$$E' \cdot P = 0$$
 (13)

where:

$$K = (k_{ij}) = k_{m-1}(x_i - x_j, y_i - y_j)$$

$$E = \begin{pmatrix} 1 & x_l & y_l & x_l^2 & x_l y_l & \dots & x_l y_l^{m-2} & y_l^{m-1} \\ 1 & . & . & . & . & . & . \\ 1 & . & . & . & . & . & . \\ 1 & . & . & . & . & . & . & . \\ 1 & x_n & y_n & x_n^2 & x_n y_n & \dots & x_n y_n^{m-2} & y_n^{m-1} \end{pmatrix}$$

$$Q' = (q_{00} \quad q_{01} \quad q_{11} \quad \cdots \quad q_{m-1m-1})$$

$$P' = (p_1 \quad p_2 \quad p_3 \quad \cdots \quad p_n)$$

$$Z' = (z_1 \quad z_2 \quad z_3 \quad \cdots \quad z_n)$$
(14)

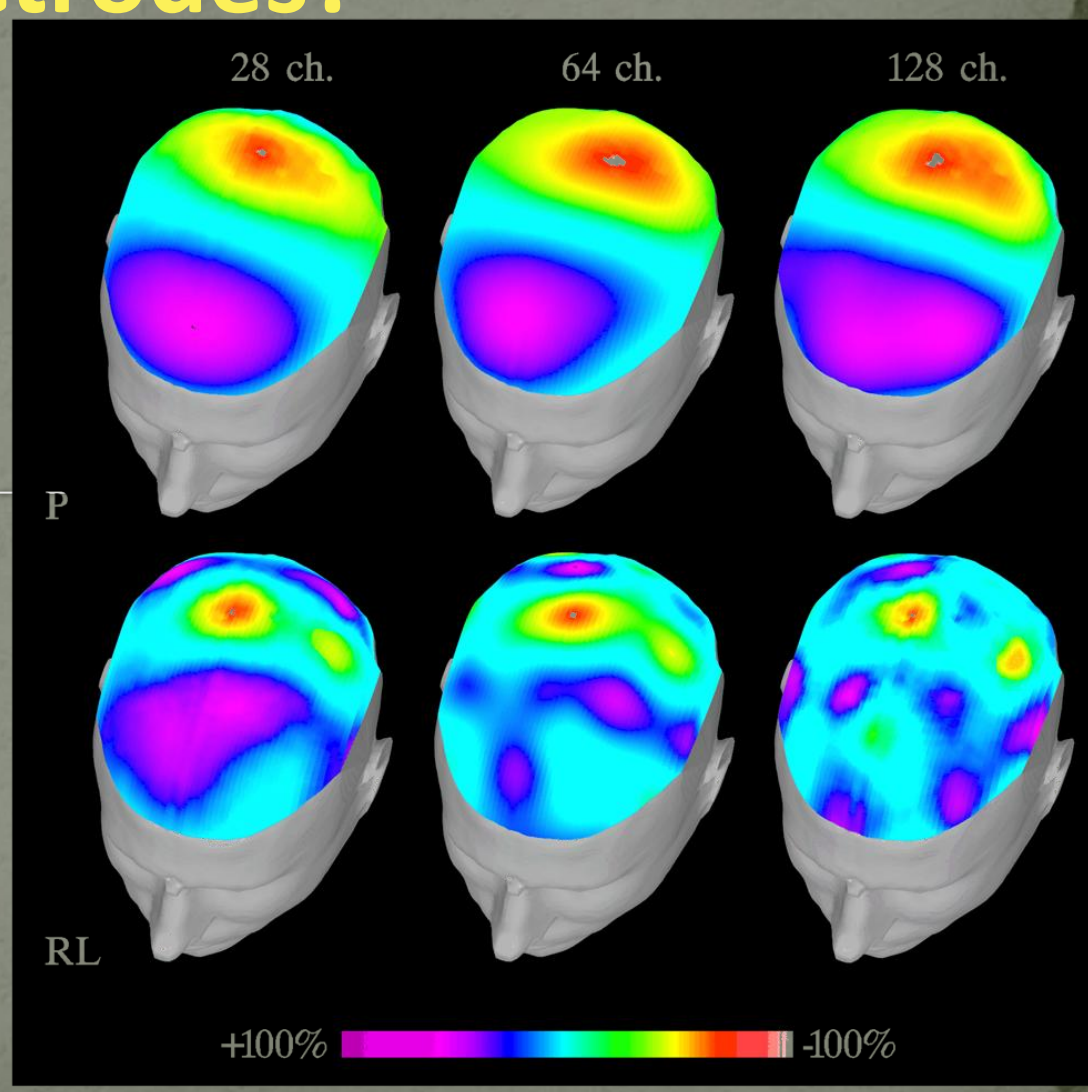
Second order thin spline and w^2 values were used to provide an infinitely differentiable model of the scalp surface. Reconstruction of the realistic scalp surface was improved using an appropriate value of ω in Eq. 13 (Harder and Desmarais, 1972; Perrin et al., 1987; Law et al., 1993). Optimal values of w^2 and ω were determined with a tuning procedure. Spherical and ellipsoidal models



Why we need to increase the number of electrodes?

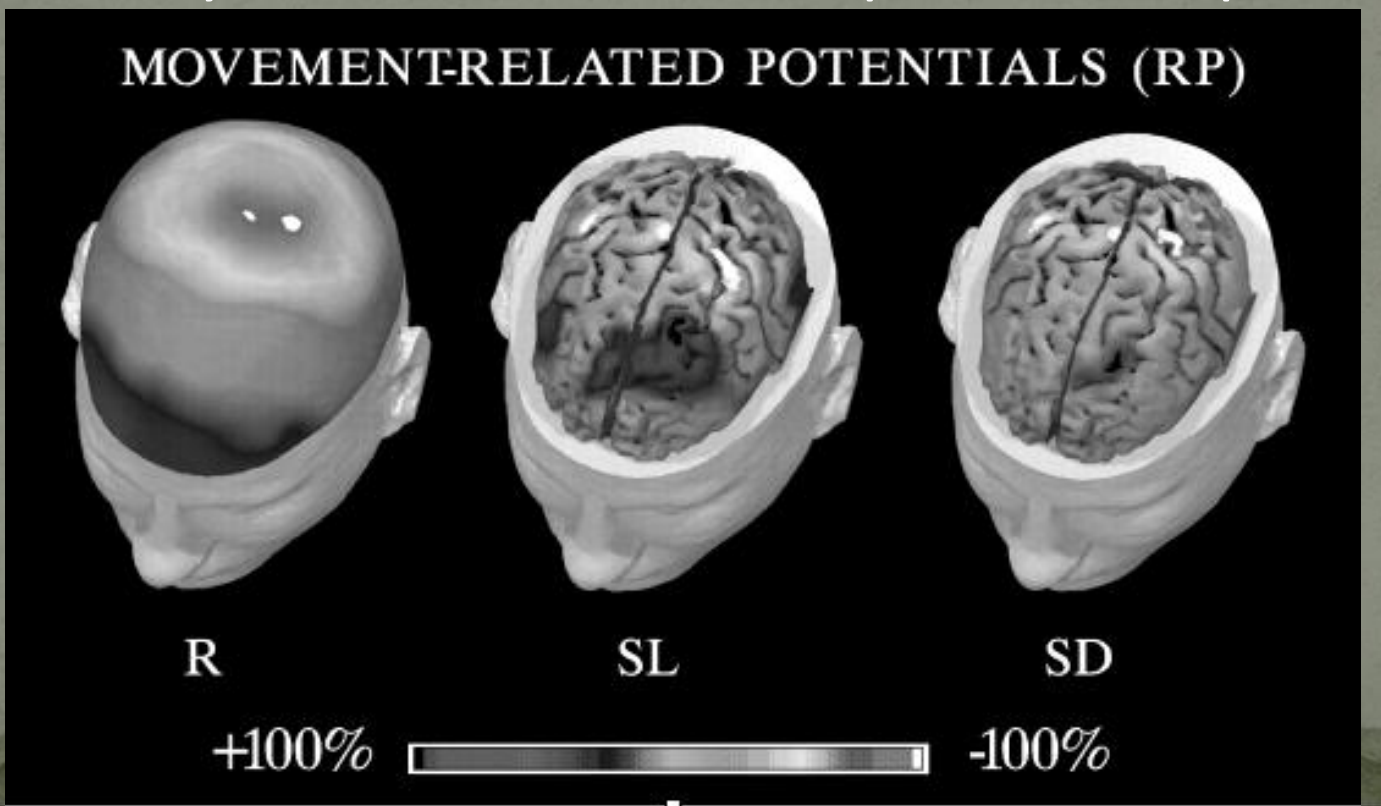
Increasing the number of electrodes do not means necessarily an increase the spatial details of the recorded EEG potential distribution

An increase of the number of electrodes more likely increase the spatial details of the SL computed distributions



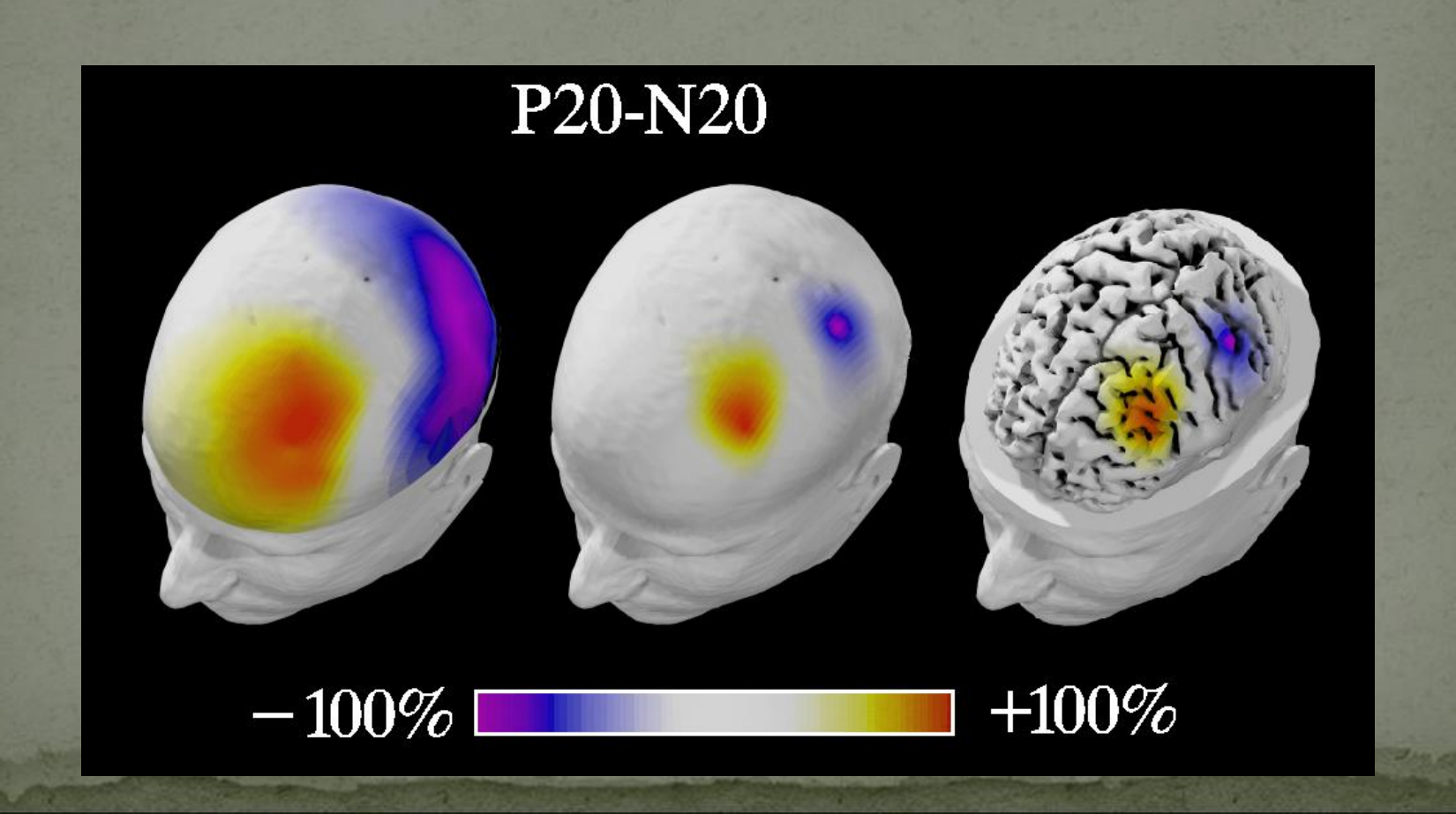
Cross validation as a supplementar validation technique

When the topography of the computed deblurred distributions are not known in advance (as in the SEP case) the comparison between the cortical activity estimated by RL and other techniques can help



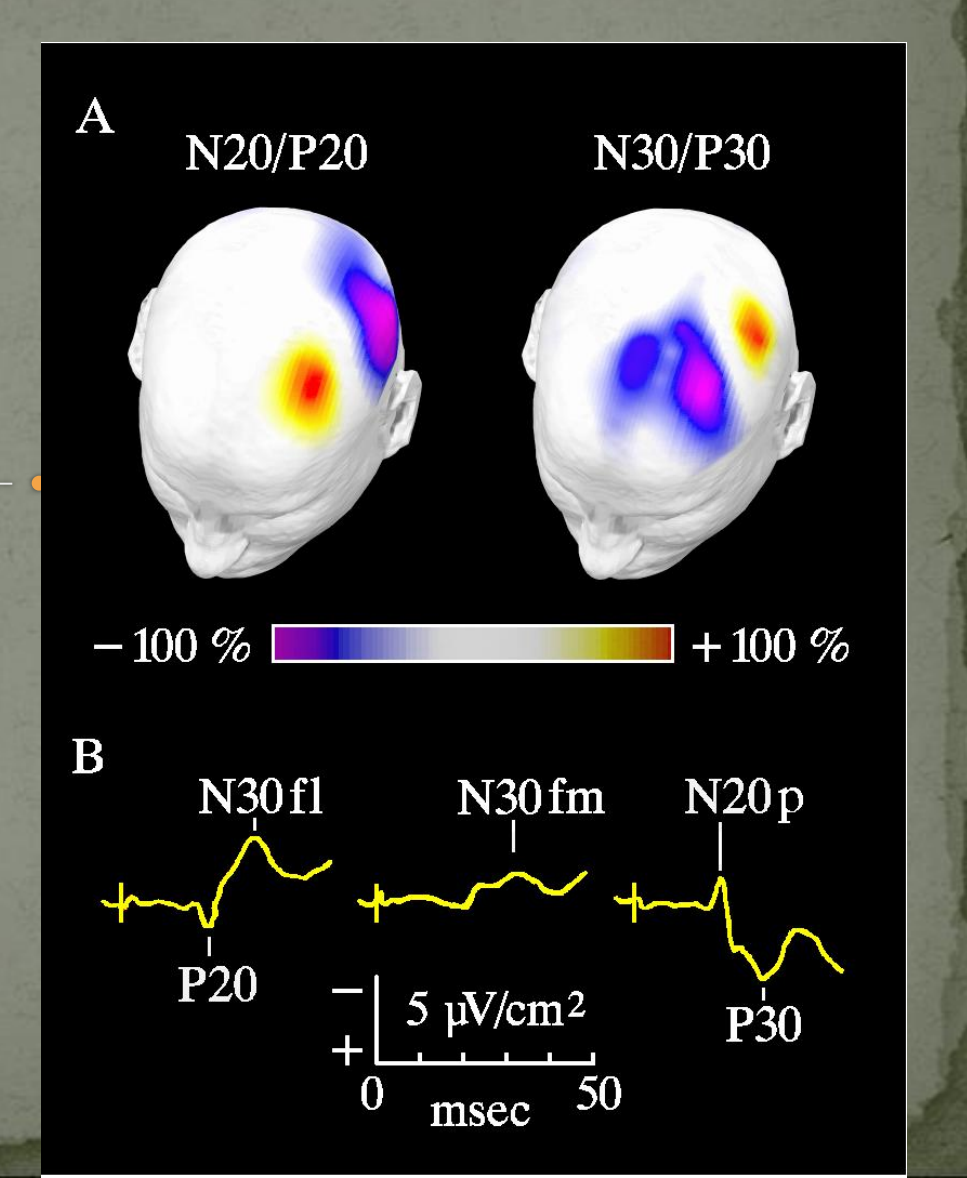
RL as a localization tool?

The RL do not aid to localize sources but rather provided reference-free and deblurred data

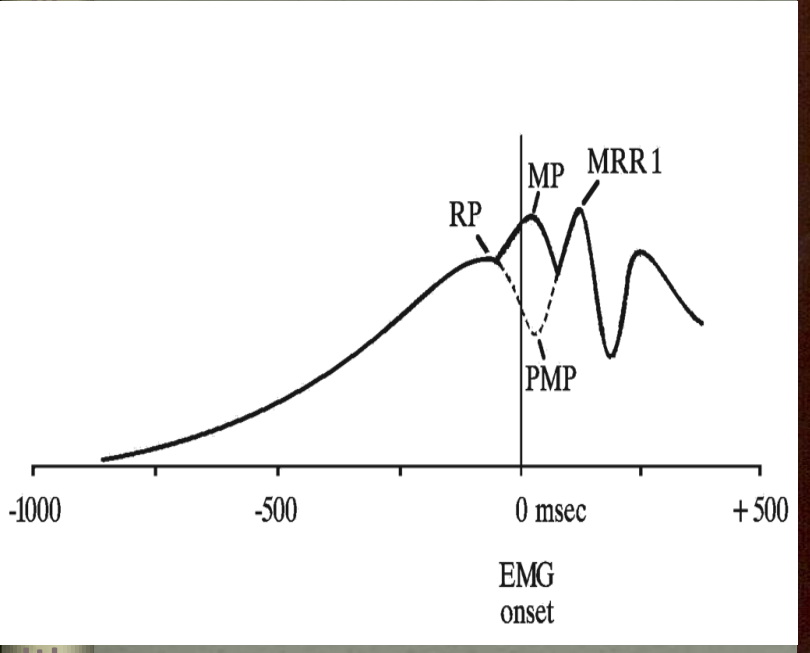


Validation of the Realistic Laplacian

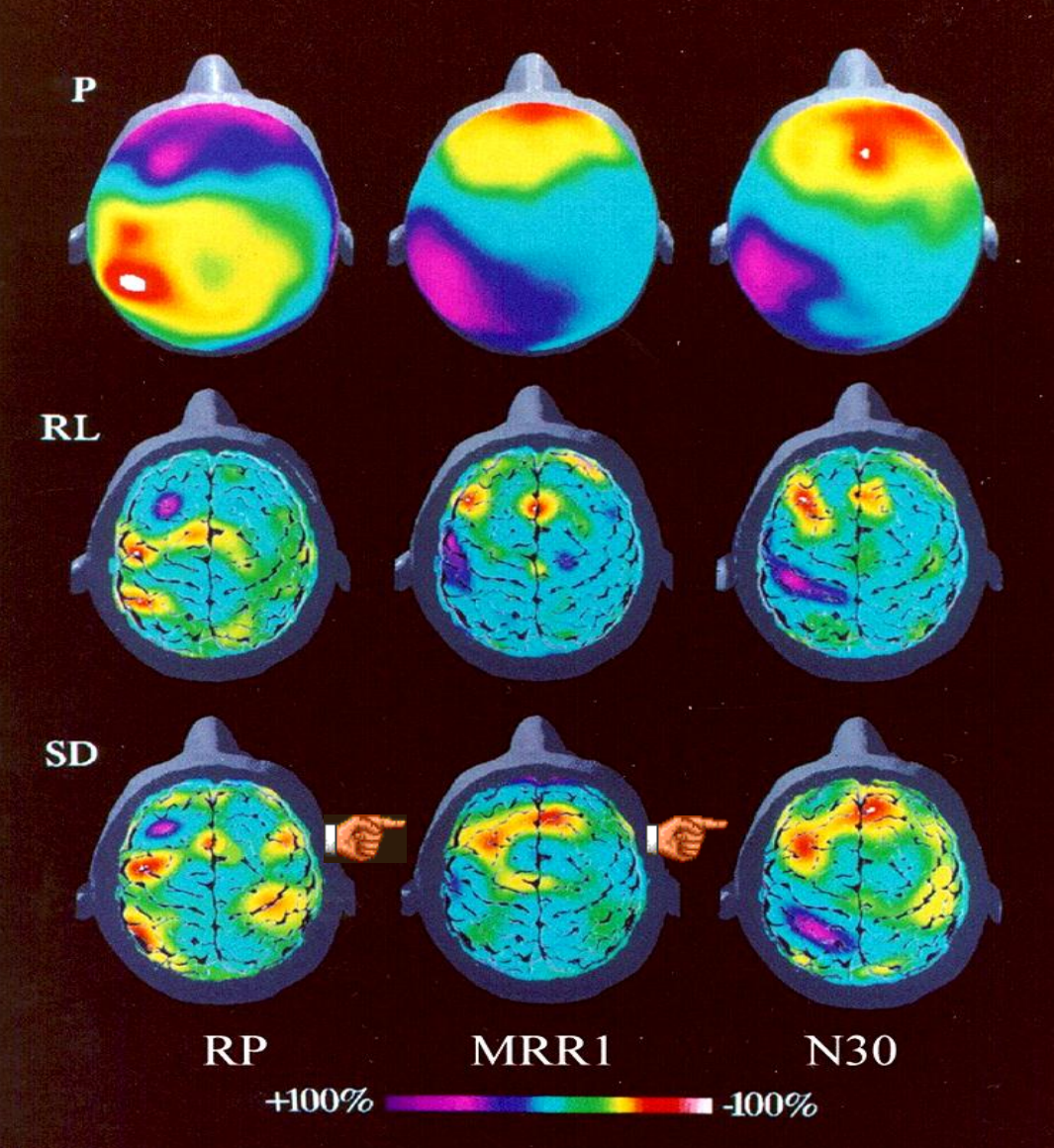
The RL can be validated if applied to potentials in which the cortical activity is known in advance as in the case of the Somatosensory-Evoked Potentials



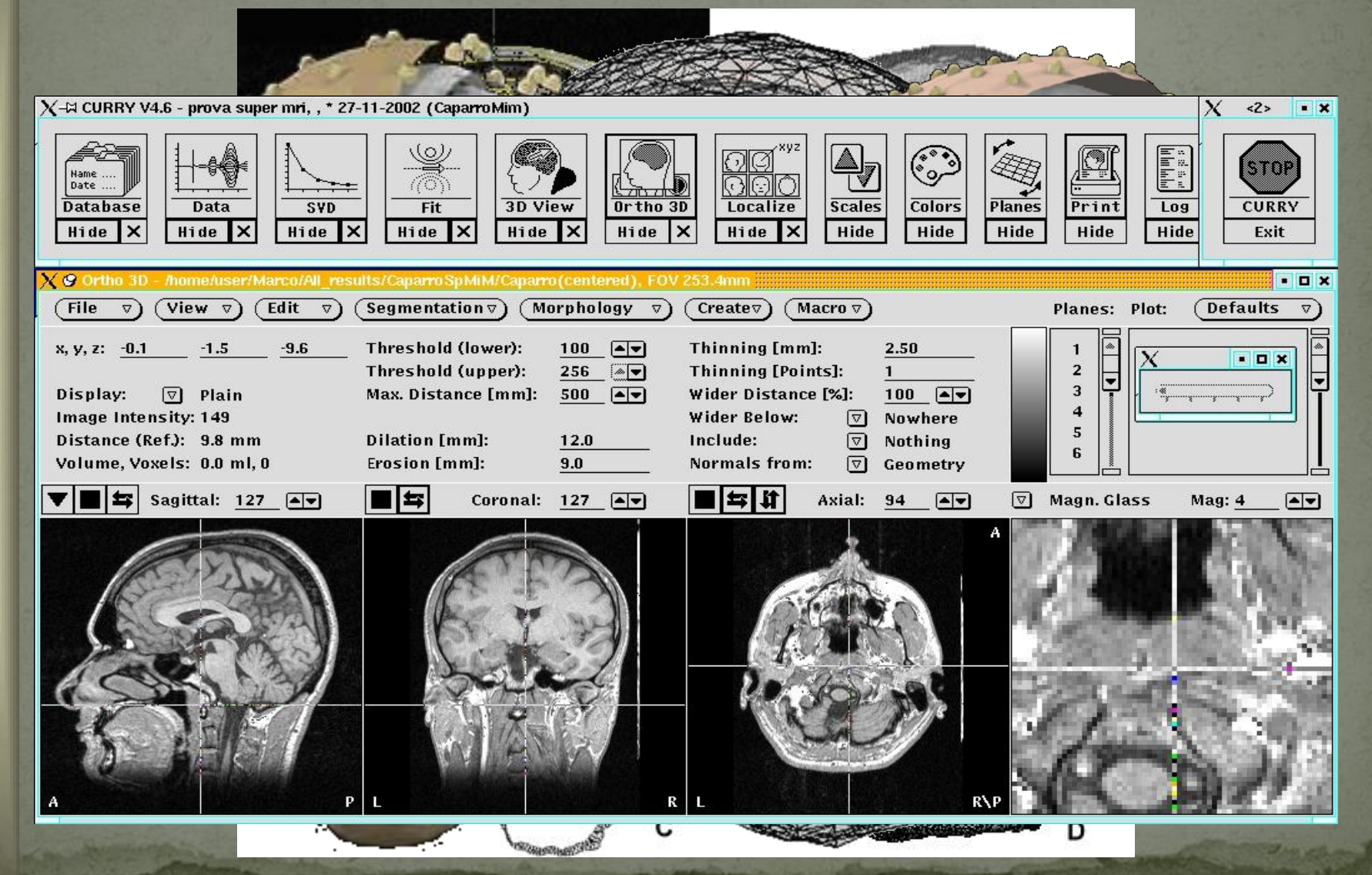
SPACE and TIME of cortical SEPs vs. movement-evoked potentials



Similar topography of movement-evoked potential (MRR1) and N30



The head as volume conductor



The subjects and their realistic head models

References for the forward problem

Pdf available from the presenter

Journal of NeuroEngineering and Rehabilitation



Review

Open Access

Review on solving the forward problem in EEG source analysis

Hans Hallez*1, Bart Vanrumste*2,3, Roberta Grech4, Joseph Muscat6, Wim De Clercq2, Anneleen Vergult2, Yves D'Asseler1, Kenneth P Camilleri5, Simon G Fabri5, Sabine Van Huffel2 and Ignace Lemahieu1

Estimate the potential generated by a current dipole in a 3D space

- Different formulations can be done, depending on the description of the medium interpose between the source (usually a dipole current) and the electrodes
- A simple structure for the head could be the sphere, in this respect the espression of the potential generated in a three layered sphere are rather simple and computable in an analytic way
- However, the head is not spherical and realistic structures have to be described by mathematical methods as Boundary Element Model, Finite Element Model and so forth
- The crucial issue is to compute the potential generated by a single dipole on the electrode array and iterates this through all the dipoles that generate our source space

Way to solve the forward problem

- Boundary Element Model (BEM)
- Finite Element Model (FEM)
- Finite Difference Model (FDM)

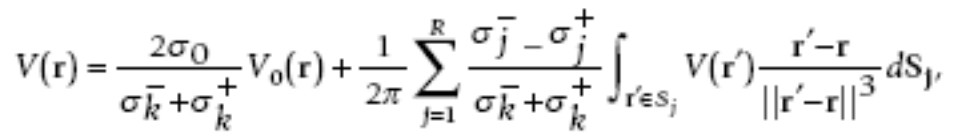
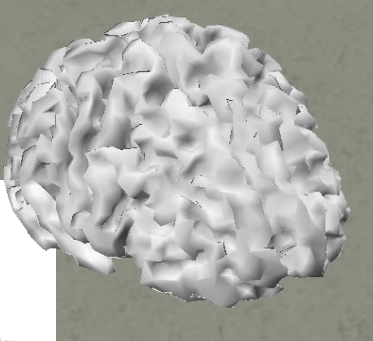
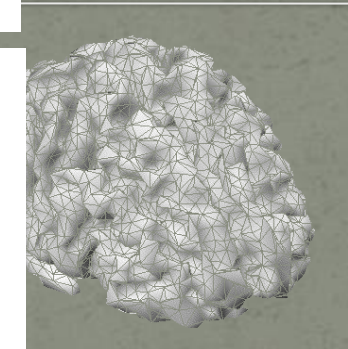


Table 2: A comparison of the different methods for solving Poisson's equation in a realistic head model is presented.

	BEM	FEM	iFDM	aFDM
Position of computational points	surface	volume	volume	volume
Free choice of computational points	yes	yes	no	no
System matrix	full	sparse	sparse	sparse
Solvers	direct	iterative	iterative	iterative
Number of compartments	small	large	large	large
Requires tesselation	yes	yes	no	no
Handles anisotropy	no	yes	no	yes



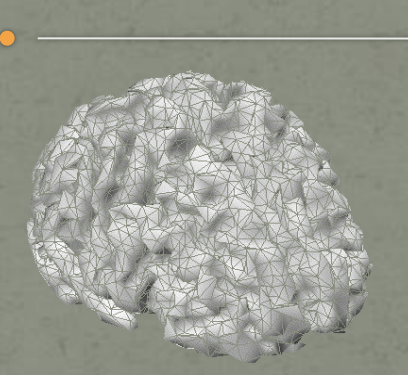




General procedure for the estimation of the lead field matrix

- Take the position of the first dipole
- It could be
 - Hortogonal to the surface
 - 3D component x,y,z
- Put the unitary value for its magnitude
- Estimate the value of the potential on the electrodes
- Put this value on a matrix A (the lead field matrix) whose dimension are Number of electrodes x number of sources

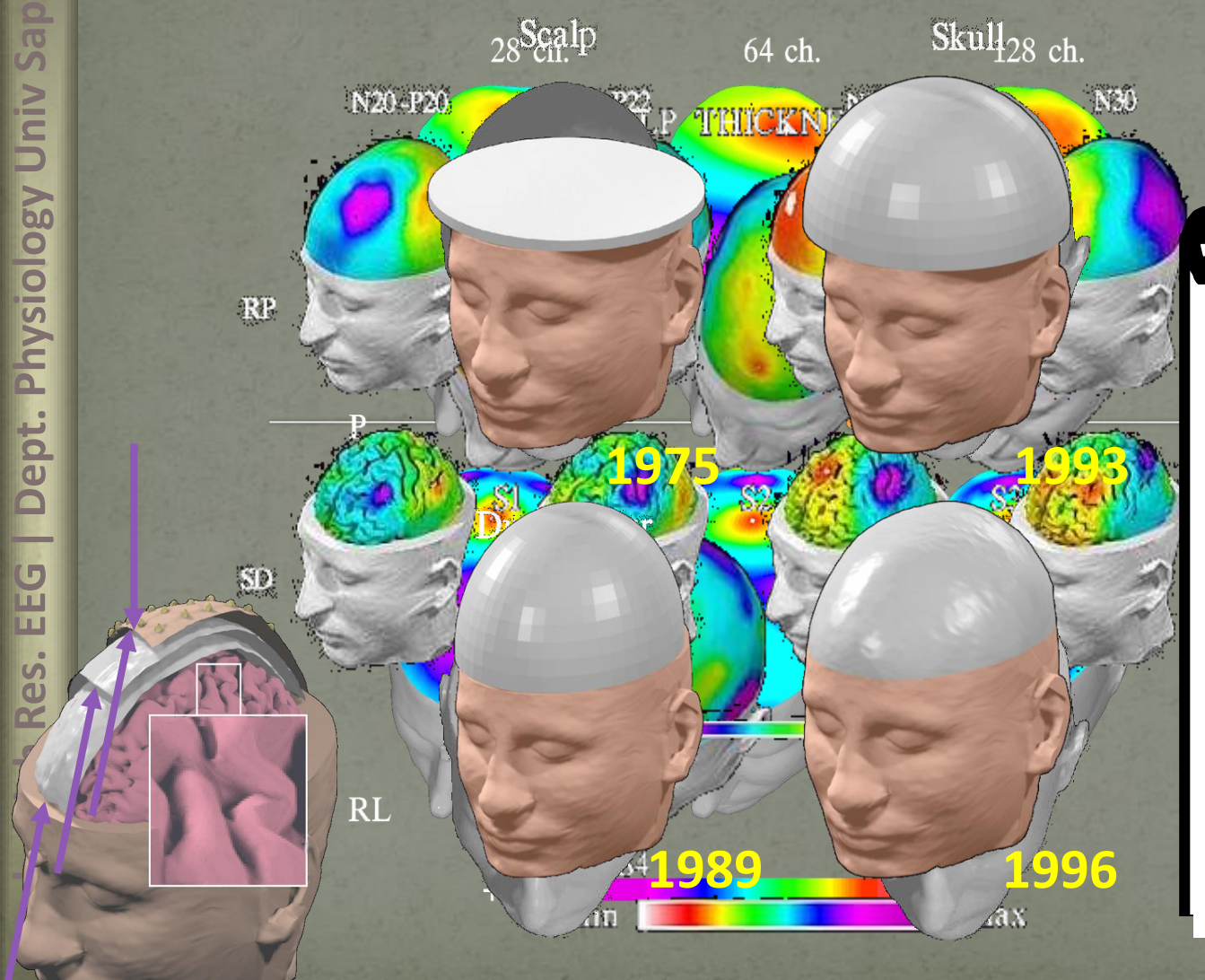






(Nelectrodes x Ndipoles)

Steps to improve the spatial details of recorded EEG Data



55555555555

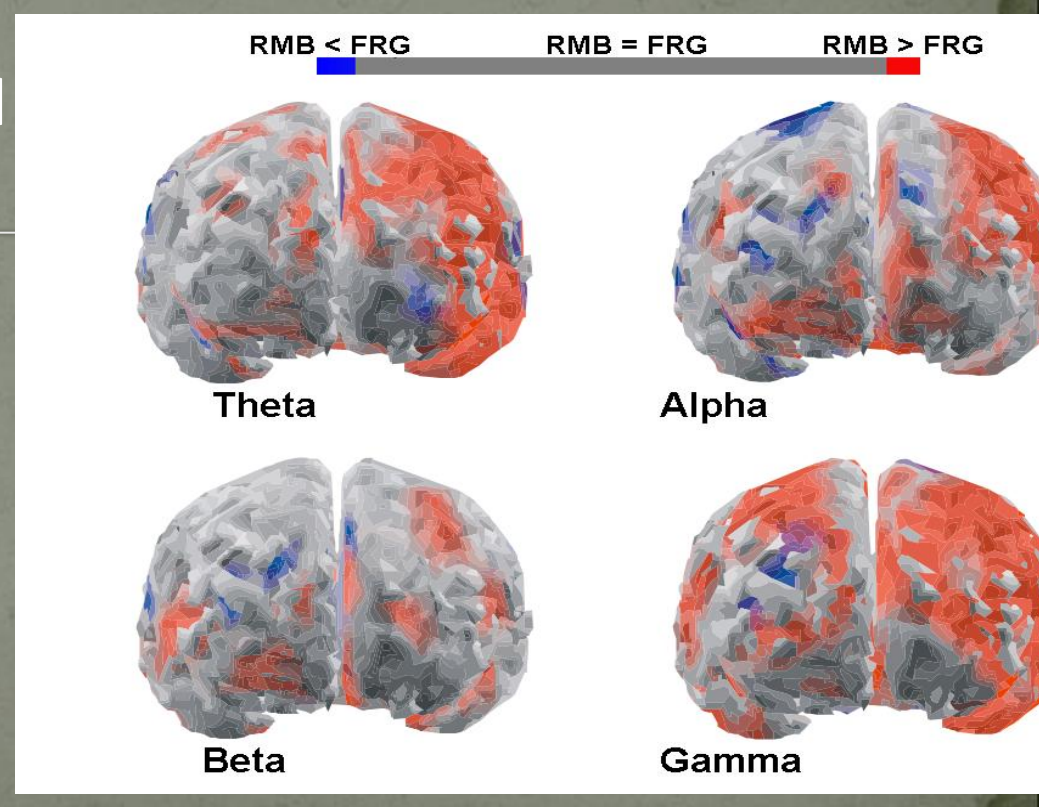
Insert the geometry of skull and dura mater in inverse calculation

Statistical analysis of high resolution EEG data

- We have the capability to estimate indexes of activity in
 - any electrode of the large arrays todays employed in high resolution EEG
 - Any voxels of the detailed source space (i.e. cortical or brain model) now available by using MRI of the subjects
- The issue now is how we could compare in two populations changes in those indexes?
- Univariate statistics (like t-Students test) are good in this respect and are generally performed at the particular level of significance (i.e. 5%)
- This means that we have a 5% of commit an error of type
 I for each test we made, i.e 5 out 100 tests we get errors
 saying that an activity is significant while it is not the case

Is this important?

- How we can protect from these type I errors, i.e saying that a difference is statistically significant at 5% level of significance while is not the case?
 - If the statistical significance is p = 0,05 and we perform 3000 tests we have a chance that some voxels became significant that it is as follows:
- 0,05 * 3000 = 150 voxels became red without by chance alone



fMRI of salmon's brain (dead) during the observation of social event

- Upper figure: Sagittal and axial images of significant brain voxels in the task > rest contrast. The parameters for this comparison were t(131) > 3.15, p(uncorrected) < 0.001, 3 voxel extent threshold.
- Two clusters were observed in the salmon central nervous system.
 One cluster was observed in the medial brain cavity and another was observed in the upper spinal column
- Lower figure Salmon results
 overlaid onto an average human
 brain in normalized space.
 Functional clusters would have
 been observed in bilateral anterior
 cingulate, left globus pallidus, right
 mid insula, and left hippocampus.

4.0 3.5 3.0 2.5 *t*-value 3.0 2.5 t-value

130,000 voxels usually employed in fMRI

Are the correction applied in fMRI studies?

- Correction percentages for multiple execution of multivariate tests were performed in NeuroImage (68%), Human Brain Mapping (80%), PNAS (44%), SCAN (33%) and Neuropsychologia (80%) all articles during February 2009 were reviewed.
- The March 2009 issue of Social, Cognitive, and Affective Neuroscience was examined. Articles for consideration from PNAS were chosen based on the January-March 2009 time frame and included 'fMRI' in the title or abstract.
- For the correction percentages in NeuroImage, Human Brain Mapping, and Neuropsychologia all articles during February 2009 were reviewed. The March 2009 issue of Social, Cognitive, and Affective Neuroscience was examined. Articles for consideration from PNAS were chosen based on the January-March 2009 time frame and included 'fMRI' in the title or abstract.
- During one poster session at a recent neuroscience conference only 21% of the researchers used multiple comparisons correction in their research (9/42)

How we can tackle this problem?

 Two widely utilized approaches are to place limits on the FWER (family-wise error rate) or the FDR (false discovery rate). The family-wise error rate represents the probability of observing one or more false positives after carrying out multiple significance tests. Using a familywise error rate of FWER = 0.05 would mean that there is a 5% chance of one or more false positives across the entire set of hypothesis tests. The Bonferroni correction is probably the most widely known FWER control and is the correction method that most investigators are familiar with.

The Bonferroni correction

- The Bonferroni correction is derived by observing Boole's inequality
- If you perform n tests, each of them significant with probability β , (where β is unknown) then the probability that at least one of them comes out significant is n β (by Boole's inequality) .
- Now we want this probability to equal α , the significance level for the entire series of tests. By solving for β , we get $\beta = \alpha / n$. This result does not require that the tests be independent.
- In our case we have α = 0,05 and β = 0,05/3000 = 0,000016
- This is the new value of significance to conclude for a statistical significance of 5% Bonferroni corrected for multiple comparisons

The possible drawback of the Bonferroni correction

- The Bonferroni correction is quite flexible in that it does not require the data to be independent for it to be effective. However, there is some consensus that Bonferroni may be too conservative for most fMRI data sets (Logan, Geliazkova, & Rowe, 2008).
- This is because the value of one voxel is not an independent estimate of local signal. It is highly correlated with the values of surrounding voxels due to the intrinsic spatial correlation of the BOLD signal and to Gaussian smoothing applied during preprocessing.
- This causes the corrected Bonferroni threshold to be unnecessarily high, potentially eliminating valid results. More adaptive methods are necessary to avoid the rejection of true signal while controlling for false positives.

Release the severity of Bonferroni correction

Controlling the FWER does the best job of limiting false positives but also comes at the greatest cost of statistical power. A second approach to multiple comparison correction is to place limits on the false discovery rate. Using a false discovery rate of FDR = 0.05 would mean that at most 5% of the detected results are false positives. See Benjamini and Hochberg (1995), Benjamini and Yekutieli (2001), and Genovese, Lazar, and Nichols (2002) for a more in-depth discussion of false discovery rate in fMRI. FDR does yield more false positives than FWER methods, but may represent a more ideal balance between statistical power and multiple comparisons control because of its less conservative approach.

A Bonferroni-Holm correction example

- Suppose that there are k hypotheses to be tested and the overall type 1 error rate is α. In our context, k could be equal to 3,000 (one t-test for each cortical dipole), and the error rate is 5%.
- Execution of the multiple univariate tests results in a list of 3,000 p-values. The issue now is how to deal with such p-values by using the Holm-Bonferroni procedure. This procedure starts by ordering the p-values and comparing the smallest p-value to α/k , the value of the Bonferroni correction to be adopted for only one p-value. If that p-value is less than α/k , then that hypothesis can be rejected and the procedure started over again with the same α .
- In our case we have α = 0,05 α * = 0,05/3000 =0,000016
- The procedure tests the remaining k-1 hypotheses by ordering the k-1 remaining p-values and comparing the smallest one to $\alpha/(k-1)$. This procedure is iterated until the hypothesis with the smallest p-value cannot be rejected. At that point the procedure stops, and all hypotheses that were not rejected at previous steps are accepted.
- In our case we have $\alpha^{**} = 0.05/2999 = 0.000016$
- This procedure is obviously less severe than the simple application of the Bonferroni test on all of the p-values with the threshold level α/k
- If all runs well the last test will be performed at p<0,05!</p>

Another example of the Bonferroni-Holm procedure

Four are tested with α = 0.05. The four unadjusted p-values are 0.01, 0.03, 0.04, and 0.005. The smallest of these is 0.005. Since this is less than 0.05/4, four is rejected (meaning some likely explains the data). The next smallest p-value is 0.01, which is smaller than 0.05/3. So, null hypothesis one is also rejected. The next smallest p-value is 0.03. This is not smaller than 0.05/2, so you fail to reject this hypothesis (meaning you have not seen evidence to conclude an alternative hypothesis is preferable to the level of α = 0.05). As soon as that happens, you stop, and therefore, also fail to reject the remaining hypothesis that has a p-value of 0.04. Therefore, hypotheses one and four are rejected while hypotheses two and three are not rejected.

Conclusions

- Surface Laplacian is an effective way to increase spatial details of the recorded EEG potentials
- Using accurate model of the volume conductor allow to estimate cortical activity from non invasive EEG recordings
- Statistics have to be applied by taking into account the difficulties that arose from the multiple execution of several univariate statistical tests

